Boundary-Layer Meteorol (2013) 146:65–80
DOI 10.1007/s10546-012-9758-x

ARTICLE

Including the Drag Effects of Canopies: Real Case Large-Eddy Simulation Studies

Pierre Aumond · Valery Masson · Christine Lac · Benoit Gauvreau · Sylvain Dupont · Michel Berengier

Received: 29 September 2011 / Accepted: 10 July 2012 / Published online: 9 August 2012

Abstract We use the mesoscale meteorological model Meso-NH, taking the drag force of trees into account under stable, unstable and neutral conditions in a real case study. Large-eddy simulations (LES) are carried out for real orography, using a regional forcing model and including the energy and water fluxes between the surface (mostly grass with some hedges of trees) and the atmosphere calculated using a state-of-the-art soil-vegetation-atmosphere-transfer model. The formulation of the drag approach consists of adding drag terms to the momentum equation and subgrid turbulent kinetic energy dissipation, as a function of the foliage density. Its implementation in Meso-NH is validated using Advanced Regional Prediction System simulation results and measurements from Shaw and Schumann (Boundary-Layer Meteorol, 61(1):47–64, 1992). The simulation shows that the Meso-NH model successfully reproduces the flow within and above homogeneous covers. Then, real case studies are used in order to investigate the three different boundary layers in a LES configuration (resolution down to 2 m) over the "Lannemezan 2005" experimental campaign. Thus, we show that the model is able to reproduce realistic flows in these particular cases and

P. Aumond (✉) · V. Masson · C. Lac
Meteo France/CNRM/GMME, Av. Gaspard Coriolis, 31057 Toulouse Cedex 1, France
e-mail: pierre.aumond@gmail.com

V. Masson
e-mail: valery.masson@meteo.fr

C. Lac
e-mail: christine.lac@meteo.fr

B. Gauvreau · M. Berengier
Ifsttar, Route de Bouaye, CS4, 44344 Bouguenais Cedex, France
e-mail: benoit.gauvreau@ifsttar.fr

M. Berengier
e-mail: michel.berengier@ifsttar.fr

S. Dupont
INRA, UR1263 EPHYSE, 33140 Villenave d'Ornon, France
e-mail: sylvain.dupont@bordeaux.inra.fr

confirm that the drag force approach is more efficient than the classical roughness approach in describing the flow in the presence of vegetation at these resolutions.

Keywords Canopy · Drag force approach · Large-eddy simulation · Meso-NH

1 Introduction

Many applications need an accurate representation of the atmospheric boundary layer in order to observe its influence on phenomena such as acoustic propagation (Aumond et al. 2012), forest fires (Pimont et al. 2006) and pollen dispersion (Chamecki et al. 2009). In order to better represent the flow dynamics in the surface layer, large-eddy simulations (LES) are performed using ever finer vertical and horizontal resolutions that reach the order of 1 m (Dupont and Brunet 2008b; Bohrer et al. 2009). In these cases, the influence of some roughness elements (e.g. trees, buildings, etc.) on the dynamics should be taken into account not only through surface schemes, as is usually done in mesoscale meteorological models, but also within the dynamic equations in the model. Instead of using the current roughness approach, a drag force approach has been implemented in several meteorological mesoscale models: MM5 (Penn State/NCAR Mesoscale Model)—Otte et al. (2004), ARPS (Advanced Regional Prediction System)—Dupont and Brunet (2008a), and RAMS (Regional Atmospheric Modeling System)—Bohrer et al. (2009).

Shaw and Schumann (1992) and Kanda and Hino (1994) have shown the potential of LES to explore airflow above and within a canopy layer by introducing the drag force approach. In parallel, many field or wind-tunnel experiments (Irvine et al. 1997; Poggi et al. 2004) have been conducted to improve our knowledge of flow statistics above and within vegetation (see Finnigan 2000 for a review) while many comparisons have also been made between observations and LES. For example, Patton et al. (1998) and Poggi and Katul (2010) compared their simulation results with wind-tunnel measurements, and Dupont and Brunet (2008a) and Dupont et al. (2008) carried out simulations including comparisons over homogeneous and heterogeneous canopy patterns. These various studies have shown the reliability of LES results when a drag force approach is used, even for complex plant canopies. However, they all represent idealized cases over flat ground or simple hills, with homogeneous cover or a regular inhomogeneous cover pattern. In the present paper, we compare LES results with a real case experiment over a large domain (up to 10 km^2). The aim is to observe the impact of the drag-force approach on the LES boundary-layer representation under different stratifications in a real case situation, i.e. over real orography, using a regional forcing model, and taking energy and mass exchange into account through a surface parametrization scheme.

The experimental campaign "Lannemezan 2005" (see Junker et al. (2006) and the description in the second section) will be used to make comparisons with a Meso-NH numerical experiment, detailed in Sect. 3. The drag-force approach is presented and implemented in Sect. 3 and its validation is given in the Appendix. Then, simulation results are evaluated and discussed, with and without the canopy scheme, in Sect. 4. Finally, Sect. 5 draws some conclusions and notes some possibilities for future work.

2 Field Experiment

"Lannemezan 2005", already presented in Junker et al. (2006), was an experiment conducted by the Laboratoire Central des Ponts et Chaussees and Electricite De France near the city

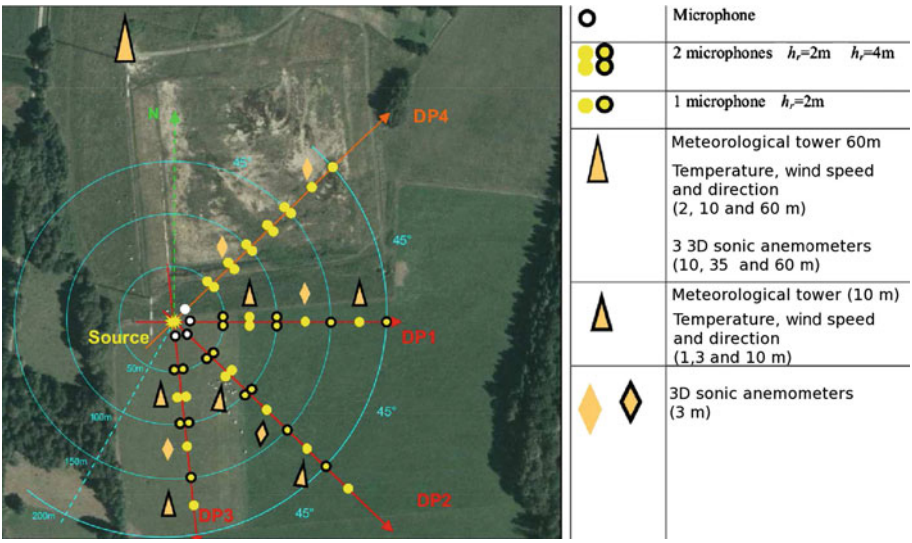

Fig. 1 Experimental protocol for acoustics and micrometeorology during the "Lannemezan 2005" experiment. The *black circled symbols* indicate the devices that were on site for the three months. Other devices were removed after three weeks. Note the presence of tree barriers on either side of the experimental domain

of Lannemezan (France). This large experimental campaign was carried out over a three-month period (in June, July and August 2005) in order to study the effect of meteorological conditions on outdoor acoustic propagation. Figure 1 shows the "Lannemezan 2005" site and the location of selected lines (DP1, DP2, DP3 and DP4) equipped with acoustic and micrometeorological devices. The "Lannemezan 2005" site was open, flat, grassy ground, with tree barriers approximately 10 m high on each side of the domain studied. This site was also chosen because of the variety of wind speeds and directions, and because of the presence of a reference weather station (Meteo-France synoptic station) nearby. The experimental protocol for acoustic and micrometeorological sensors is summarized in Fig. 1 and more details are provided in Junker et al. (2006). About 50 microphones were set up along the four propagation directions (DPi). The micrometeorological devices comprised, 3D ultrasonic anemometers (YOUNG and CAMPBELL CSAT1 with a 20Hz sampling rate) located 125 m from the source in each propagation direction (DPi) at 3 m above the ground. The 10-m high meteo towers (75 and 175 m from the source on each DP) were fully equipped with wind speed, wind direction and air temperature (YOUNG sensors with a 10 s sampling rate) located at 1 m, 3 m and 10 m above the ground. An additional 60-m high meteorological tower equipped with 3 YOUNG ultrasonic anemometers, 3 YOUNG temperature sensors and 3 YOUNG humidity sensors was located 200 m north of the source (measuring heights: 10 m, 35 m, 60 m) and were in operation throughout the three-month period. Thus a total of 70 micrometeorological sensors were operated during the "short" (and intensive) monitoring period. All the meteorological data were next filtered, validated, averaged and post-processed so as to give turbulent kinetic energy (TKE) information on 15-min meteo samples during the 3-month period Junker et al. (2006). In order to validate the meteorological model, three typical clear-sky conditions were chosen in the experimental database from the Lannemezan 2005 experiment. The dimensionless stability parameter ς was chosen to define the degree of stratification, and was calculated from averaged sonic

anemometer measurements. The three days chosen were: 17 June during daytime, corresponding to unstable conditions ($\varsigma = z/L \simeq -0.3$), 3 July during nighttime, corresponding to very stable conditions ($\varsigma = z/L \simeq 0.3$), and 16 June during nighttime, presenting neutral-stable atmosphere characteristics ($\varsigma = z/L \simeq 0.1$). Here, z is the height and L is the Obukhov length.

3 Numerical Experiment

3.1 Model

Meso-NH (Lafore et al. 1998) is the non-hydrostatic mesoscale atmospheric model of the French research community. It is intended to be applicable at scales, ranging from large (synoptic) scales to small scales (LES). The model uses a 1.5-order turbulence scheme, with two different mixing length parametrizations (Deardorff 1980; Bougeault and Lacarrere 1989; Cuxart et al. 2000a); its performance has been tested successfully for several boundary-layer regimes (Cuxart et al. 2000b; Jiménez and Cuxart 2005; Tomas and Masson 2006). In this work, we present a nested LES approach for a real case study, i.e. over real orography and taking interactive surface-atmosphere exchange into account through a surface parametrization scheme. Furthermore, the large-scale information was provided by a regional model, down to the LES resolution, through the grid nesting over the sub-domain of interest. Only a few examples exist of this original approach, notably the experiments conducted by Chow et al. (2006), Weigel et al. (2006, 2007) in a narrow, steep Alpine valley at 150-m resolution. In large-scale atmospheric models, the effects of the canopy on flow are usually parametrized using a roughness approach. However, in LES on a real site, the complexity of the dynamic variable profiles within the canopy is not well represented by this method: trees are high enough to cross several atmospheric layers, and the LES horizontal resolution would be good enough to represent the wake circulation behind the tree barriers, necessitating a more realistic parametrization of the influence of the obstacles on the near-surface flow. One solution is to use a drag force approach, which consists of adding terms in the model dynamic equations to express the effects of trees on the flow. A detailed description of the basic equations of the Meso-NH model is available in Lafore et al. (1998) and only the new canopy parametrization formulation, a drag-force approach, is described below.

Thus, in order to represent the effects of drag due to the canopy elements on the flow, an additional term is added to the momentum equations:

$$\frac{\partial u}{\partial t} = Adv + Cor + Pres + Turb(u) - C_{\mathrm{d}} A_{\mathrm{f}}(z) u (u^2 + v^2)^{0.5}, \tag{1}$$

$$\frac{\partial v}{\partial t} = Adv + Cor + Pres + Turb(v) - C_{\mathrm{d}} A_{\mathrm{f}}(z) v (u^2 + v^2)^{0.5}, \tag{2}$$

where u, v are the two horizontal wind components in m s^{-1}, C_{d} is the canopy drag coefficient and $A_{\mathrm{f}}(z)$ in m^{-1} is the canopy area density (a function of the height above the surface z), Adv denotes advection terms, Cor denotes the Coriolis force term, $Pres$ indicates the pressure gradient term, and $Turb$ indicates the turbulence term. In this study, the drag force in the vertical direction is neglected, assuming that all leaves are oriented in the vertical plane (i.e. no frontal area in the vertical direction). Although the performance obtained with the present model is good (see Appendix), we plan to include a vertical drag force in a future version of our model.

In addition, trees have an effect on small-scale turbulence. Because leaves are much smaller than the scale of the grid mesh, they produce additional very small-scale motions, and hence additional dissipation (Kanda and Hino 1994; Shen and Leclerc 1997; Patton et al. 2003). We follow these authors to parametrize this additional dissipation in the TKE:

$$\frac{\partial e}{\partial t} = Adv + DynProd + ThermProd + Turb + Diss - C_{\mathrm{d}} A_{\mathrm{f}}(z) e (u^2 + v^2)^{0.5}, \quad (3)$$

where e is the subgrid-scale TKE in $\mathrm{m}^2\,\mathrm{s}^{-2}$, and Adv denotes the advection of TKE, $DynProd$ denotes the dynamic production, $ThermProd$ is the thermal production, $Turb$ is the turbulent transport of TKE and $Diss$ is the dissipation.

The canopy area density $A_{\mathrm{f}}(z)$, represents the surface area of the trees facing the flow per unit volume of canopy, and it represents the variation of drag on the wind and the TKE dissipation due to the density of leaves in the trees. It is a combination of A_i, the product of the fraction of vegetation in the grid cell, by the leaf area index (LAI), and a weighting function that represents the shape of the trees.

Some other assumptions or approximations can also be made:

- The canopy also influences thermodynamics. As a first approximation, the canopy fluxes are only represented by the vegetation surface scheme [interaction soil–biosphere–atmosphere (ISBA) presented in Noilhan and Planton (1989)].
- It is also considered that the volume lost due to the presence of trees does not modify the air volume in the grid cell.
- Wake generation by leaves is neglected because it has been found to have only small effects on the total TKE (Shaw and Schumann 1992).

The validation of this model implementation in Meso-NH is presented in the Appendix.

3.2 Model Configuration

Simulations were carried out using three grid-nested $200 \times 200 \times 80$ grid points centered around the area of the "Lannemezan 2005" site (see Sect. 2). The domain size ($10 \times 10\ \mathrm{km}^2$) was chosen in order to include the largest scale eddies. LES were performed with horizontal resolutions of 50 m, 10 m and down to 3.3 m in order to resolve the smallest eddies. A vertical terrain-following stretched grid was used. These grids contained 50 vertical levels in the first 100 m (from a 1-m near-ground resolution). Table 1 gives a synthesis of these different model configurations. For the unstable case, it can be noted that the largest eddies are typically as large as the boundary-layer depth and are well resolved at a 50-m horizontal resolution. In this way, the Deardorff mixing length was selected for grids at 50 and 10 m and the third grid was considered unnecessary; and so the third model did not contribute further information. Surface parameters (tree height, LAI, density of trees, etc.) were provided by the ISBA model. The height of the trees was set to 10 m by the ISBA model, which was approximately the height measured in situ. The vertical distribution of frontal area density A_{f} is presented in Fig. 2. The drag coefficient C_{d} chosen was the same as in the Appendix. The land-cover positioning was deduced from interpolation of the Corine database (Büttner et al. 2004) with a horizontal resolution of 250 m except for the "Lannemezan 2005" field experiment where the data were completed manually using a numerical terrain model at 1-m resolution in order to better describe the topography and the position of trees. The position of high vegetation used for "Lannemezan 2005" is shown in Fig. 3. A Rayleigh damping layer was used at the top of the domain to absorb upward-propagating wave disturbances and to eliminate wave reflection at the boundary. The clear-sky conditions for the three days obviated the need to use a microphysical scheme. To initialize the simu-

Table 1 Configuration of the nested models

Day	Grid	First	Second	Third
16 June	Resolution (m)	50	10	3.3
	Domain size ($x \times y \times z$)	$200 \times 200 \times 80$	$200 \times 200 \times 80$	$450 \times 300 \times 80$
	Timestep (s)	0.5	0.1	0.02
	Mixing length	BL89	BL89	DEAR
	Simulated time (s)	3600	3600	900
3 July	Resolution (m)	50	10	3.3
	Domain size ($x \times y \times z$)	$200 \times 200 \times 80$	$200 \times 200 \times 80$	$450 \times 300 \times 80$
	Timestep (s)	0.5	0.1	0.02
	Mixing length	BL89	BL89	DEAR
	Simulated time (s)	3600	3600	900
17 June	Resolution (m)	50	10	
	Domain size ($x \times y \times z$)	$200 \times 200 \times 80$	$200 \times 200 \times 80$	
	Timestep (s)	0.5	0.1	
	Mixing length	DEAR	DEAR	
	Simulated time (s)	3600	3600	

DEAR Deardorff mixing length, *BL89* Bougeault–Lacarrere mixing length

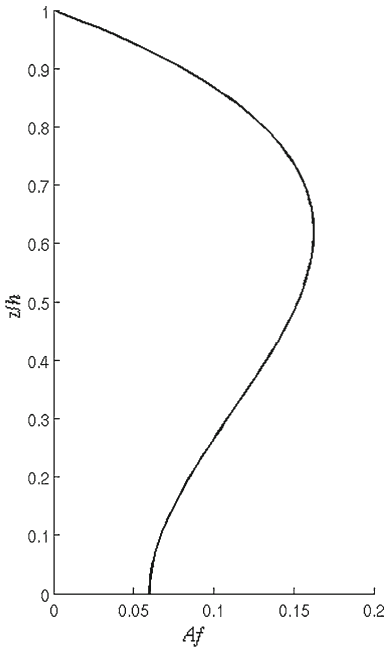

Fig. 2 Normalized frontal area density profile $A_f(z)$ multiplied by C_d; h is the height of the trees

lations, a vertical profile was interpolated over the whole domain using measurements from the 60-m tower and analysis of the regional model ARPEGE (Déqué et al. 1994) above that height.

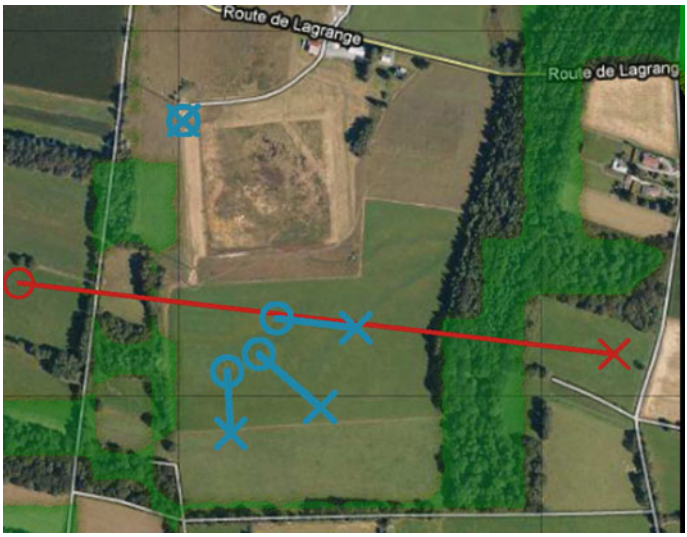

Fig. 3 "Lannemezan 2005" experiment. In *blue* sensor positioning lines (cf. Fig. 1), in *red* vertical cross-section position, *bright green areas* tree cover

Simulations were run for both the drag-force and roughness approaches, and the canopy heights chosen were 0.1 m for grass and 10 m for trees. Three different cases were studied: flow with neutral, stable and unstable stratification. The vertical profiles presented in Figs. 5, 7 and 10 were used to evaluate the model accuracy. These statistical profiles were deduced from a space-time averaging procedure using instantaneous wind velocity collected, (1) at the mast locations, and (2) every second during a 450-s period after the flow had reached an equilibrium state.

4 Results

The scientific question here is whether or not the drag force is superior to the classical roughness length approach for LES studies over such inhomogeneous terrain. Therefore, the objective of this section is to show the impact of the drag-force approach in LES under different stratifications. Firstly, the results are presented qualitatively with horizontal and vertical cross-sections (see Fig. 3 for the vertical cross-section position). The instantaneous wind fields seem to be adequate to demonstrate the impact of the drag force in the domain. However, to quantitatively compare the simulation results with the experiment, the vertical profiles of mean wind, temperature and TKE at the different measurement points need to be evaluated. In this way, because the fields are sufficiently homogeneous in time and space over the different measurement points, mean vertical profiles are proposed.

4.1 16 June 2005—Night: Near-Neutral Atmosphere

On the night of 16 June 2005, the atmospheric boundary-layer condition was quite neutral ($|\varsigma| \leq 0.1$). The flow was from the south-west of the domain and reached the measurement

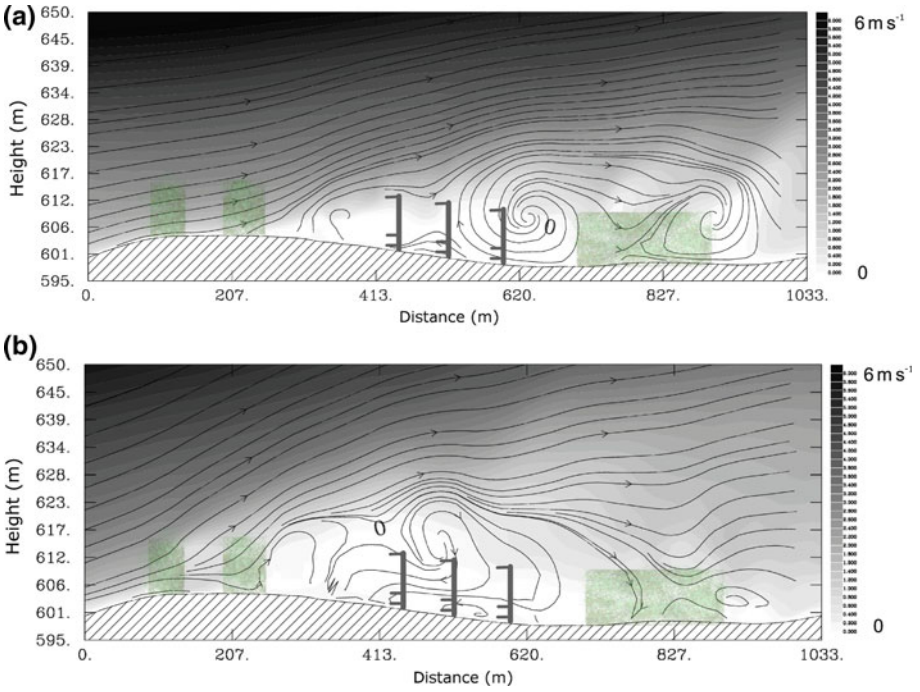

Fig. 4 Instantaneous vertical cross-section of wind speed during near-neutral conditions near tree barriers (*green areas*) over the main domain of "Lannemezan 2005" using the roughness approach (**a**) and the drag-force approach (**b**)

sensors after passing through the 10-m high tree barriers. In Fig. 4, it is possible to see the drag of the wind within and beyond the tree barriers. In this case, it can be observed that the drag-force approach has an impact around 20 m higher than the roughness approach. Moreover, this view suggests that turbulence from trees presented in the covering nested domain is not represented despite their possible impact on the main domain (for example, by adding missing TKE). The domain begins only 50 m before the first tree barrier, while the plume size reaches nearly 200 m.

Figure 5 also demonstrates the positive effects of the drag-force implementation on the flow representation. The wind-speed magnitude appears to be in better agreement with measurements and the simulated inflection point, present at 10 m (height of the trees), is close to the experimental results. Moreover, the vertical gradient of temperature is better represented. Finally, the simulated TKE is nearer to the measurements when the drag-force approach is used.

4.2 3 July 2005—Night: Stable Atmosphere

On the night of 3 July 2005, the atmospheric boundary layer was stable ($\varsigma \simeq 0.3$), and the simulations show a non-turbulent flow from the south-east. In Fig. 6, it is possible to observe the strong impact of the drag force on the flow behaviour. As for the 16 June simulation, the plume size generated by the drag-force approach led us to assume that a larger domain would be useful to accurately compare our results with the experiments. Thus, the lack of TKE

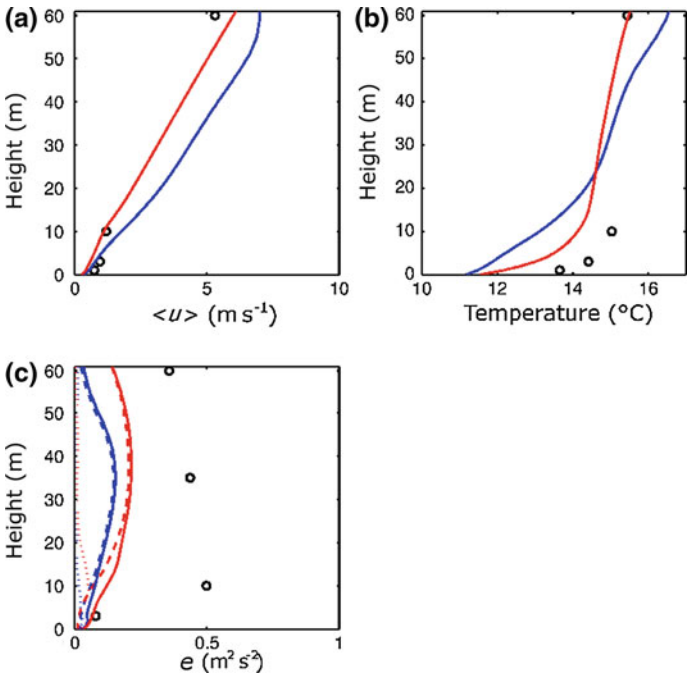

Fig. 5 Comparison for near-neutral conditions of the Meso-NH model with the roughness approach (*blue*) and the drag-force approach (*red*) against measurements (*black*) (Junker et al. 2006). Vertical profiles of mean horizontal wind speed; temperature; and subgrid (*dashed line*), resolved (*dotted lines*) and total TKE (*solid line*)

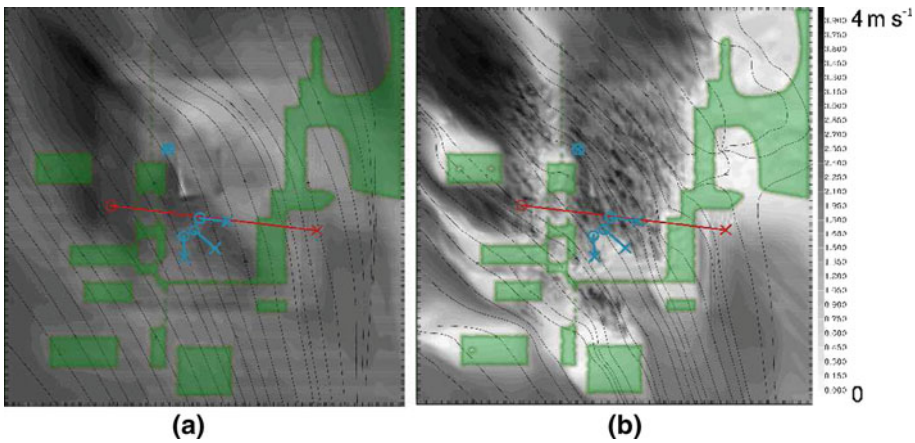

Fig. 6 Instantaneous horizontal cross-section (5-m height) of wind speed during stable conditions near tree barriers (*hatched areas*) over the main domain of "Lannemezan 2005" using the roughness approach (**a**) and the drag-force approach (**b**)

around 50-m height seen in the simulation results could be explained by the fact that TKE generated by trees outside the small domain is not represented. On the other hand, below 25 m, the TKE is too large compared with experimental results. This discrepancy can easily be

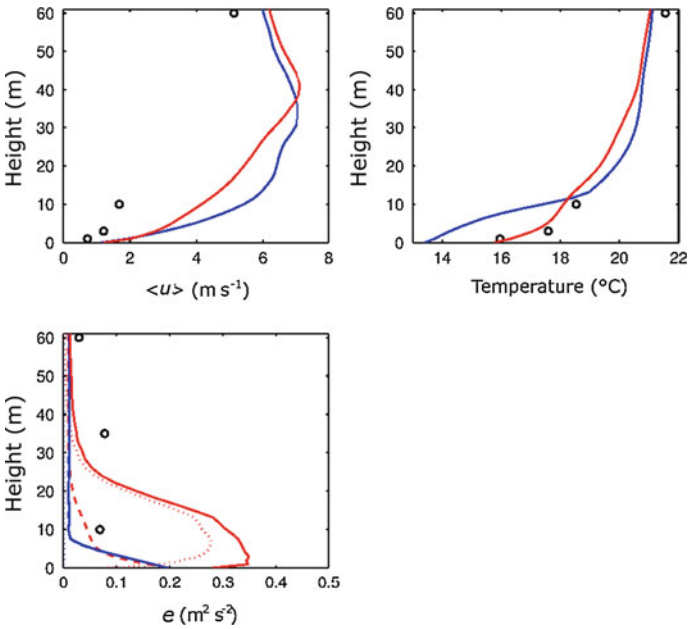

Fig. 7 Comparison, in stable conditions, of the Meso-NH model with the roughness approach (*blue*) and the drag-force approach (*red*) against measurements (*black*) (Junker et al. 2006). Vertical profiles of mean horizontal wind speed; temperature; and subgrid (*dashed line*), resolved (*dotted lines*) and total TKE

explained by the presence of an elevated simulated wind speed, shown in Fig. 7, resulting in the production of excess turbulence in the wake. Correction of this bias should provide better results. The simulation accuracy is weaker than for the near-neutral case, as shown by the excessive wind speed for example. However, it is well-known that stable conditions are difficult to simulate and only rarely do models treat them properly. The origin of this deviation may lie in an initialization bias from the large-scale model. Nevertheless, the representation of the temperature gradient is strongly improved and Fig. 7 shows the positive impact of the drag-force approach.

Another way to see the difference between the two approaches is to compare the spatial spectra of zonal wind (west–east) on the main domain (Fig. 8). In the drag-force approach, there is an energy production in the range 200–30 m, and the classic $-5/3$ slope can be observed in the two inertial zones. In the roughness length approach, it is also possible to observe energy accumulation in the dissipation range (wavelength $\sim 2\Delta x$) corresponding to numerical energy. These spectra provide confirmation that the creation of turbulence is directly correlated with the presence of trees, as taken into account by the drag-force approach.

4.3 17 June 2005—Day: Unstable Atmosphere

17 June 2005 was a sunny summer day and during daytime, the atmospheric boundary layer was quite unstable ($\varsigma \simeq -0.3$). The flow was from the west and was strongly turbulent before reaching the trees (Fig. 9). The energy gain by convection was much larger than the energy gain by shear production. As expected, the influence of the drag force of the trees

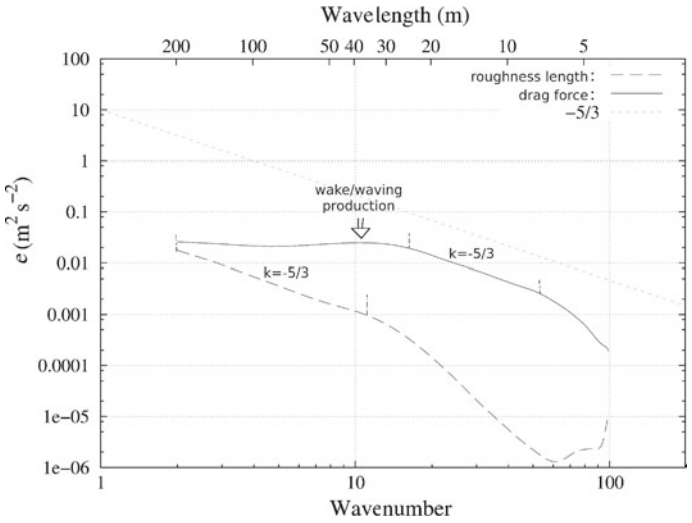

Fig. 8 Spatial spectra of zonal wind on the main experiment domain with the drag-force approach (*dotted line*) and roughness length approach (*dashed line*)

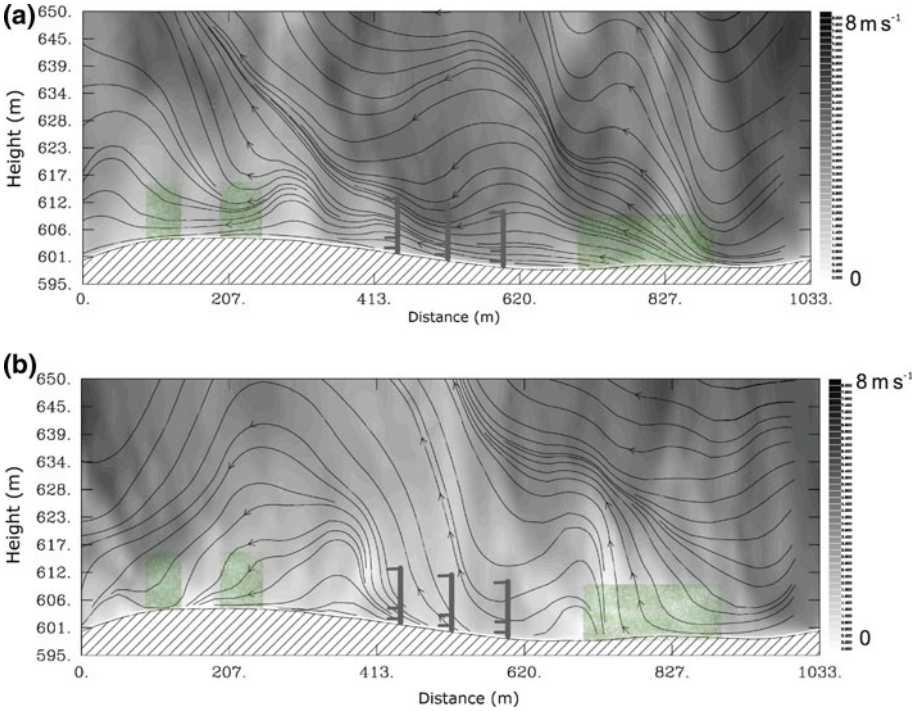

Fig. 9 Instantaneous vertical cross-section of wind speed during stable conditions near tree barriers (*green areas*) over the main domain of "Lannemezan 2005" using the roughness approach (**a**) and the drag-force approach (**b**)

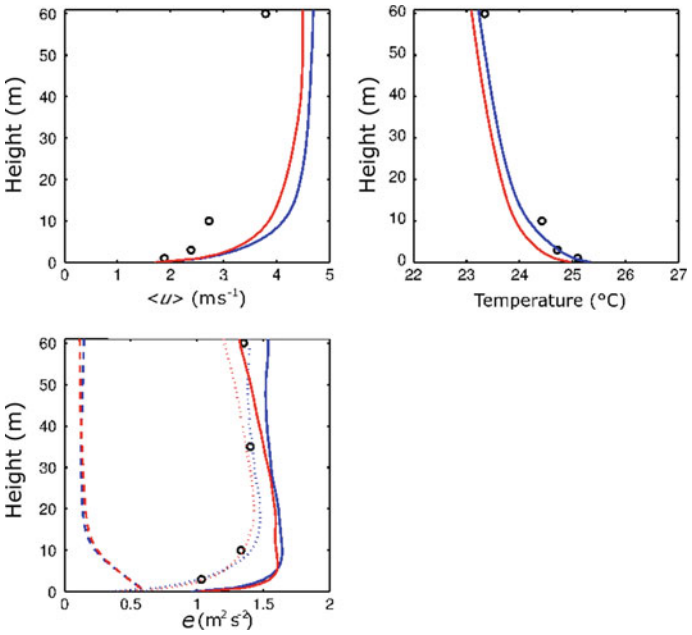

Fig. 10 Comparison, in unstable conditions of Meso-NH model with the roughness approach (*blue*) and the drag-force approach (*red*) against measurements (*black*) (Junker et al. 2006). Vertical profiles of mean horizontal wind velocity; temperature; and subgrid (*dashed line*), resolved (*dotted lines*) and total TKE

was inconspicuous and the quantitative observation confirmed this hypothesis (Fig. 10). In contrast, the vertical cross-section presented in Fig. 9 shows that, inside and just behind the trees, the drag force had an impact on the flow. The absence of measurements at this place during the campaign meant that no information was available on the quality of the flow description. However, considering past studies, we can assume that the drag force approach improved the description. It is also worth noting that no negative effects were observed on the main study (see Fig. 10).

5 Conclusion

We have presented the implementation of the drag force due to trees in the Meso-NH model, its validation and its application in real case studies. Three different boundary-layer regimes have been investigated. In stable and neutral conditions, the drag-force approach shows better model accuracy in representing the flow within and beyond the canopy compared with the classical roughness length approach. In unstable conditions, because of the pre-existing strong turbulence, the improvement was negligible. The computation time required by the drag-force method is small, so this approach is useful in real case simulations whenever the vertical resolution is finer than the vegetation height. In order to complete this study, it would be of value to use a larger domain to confirm the assumptions about the influence of trees present outside the small domain considered here. The next step could be to add the thermodynamic effects of trees by taking the trees into account in a microscale meteorological model.

Appendix: Drag-Force Validation

In order to validate the model predictions, the same simulation set-up was chosen as in Shaw and Schumann (1992), Su et al. (1998) and Dupont and Brunet (2008a). It consisted of carrying out three-dimensional simulations over homogeneous continuous forest canopies in a dry neutral atmosphere. The results were compared with measurements from Su et al. (1998) within and above a deciduous forest at Camp Borden in Ontario, Canada.

Model Configuration and Numerical Details

The simulation domain was 200 × 100 × 65 grid points covering an area of 400 × 200 m^2, and thus corresponding to a horizontal resolution of 2 m. A stretched vertical grid was used with 50 levels in the first 100 m. The domain size was chosen in order to resolve the large-scale eddies. As the horizontal grid had elements of the order of 1 m, the Deardorff mixing length was used (Deardorff 1980; Cuxart et al. 2000a). The timestep was 0.03 s, and the height of the forest was 18 m. The forest canopy had a LAI of 2, and the vertical distribution of frontal area density (A_f) is presented in Fig. 2. The value of the dimensionless drag coefficient C_d is not well known as it can depend on the type of forest or trees and can change with the flow velocity as shown by Mayhead (1973). It can take different values from 0.075 to 0.5 (Kanda and Hino 1994; Masson and Seity 2009). For simplicity, C_d is considered constant here and is set at 0.2, one of the most common values found in the literature (Dupont and Brunet 2008a; Cassiani et al. 2008). A roughness length was assigned to the surface to represent the grass under the trees, and a dry, neutral (297 K) atmosphere was used to initialize the model. In addition, the flow was driven by a height invariant geostrophic wind corresponding to the base state wind at the top of the domain (zonal wind at 18.5 m s^{-1}). In order to initialize the turbulence, noise of amplitude 1 K was set on the initial potential temperature. The surface momentum fluxes were treated by the ISBA scheme and the heat fluxes were set to zero in order to remain in neutral conditions. The lateral boundary conditions were periodic and a Rayleigh damping layer was used at the top of the domain to absorb upward-propagating wave disturbances and to eliminate wave reflection at the boundary.

Results

After the flow had reached an equilibrium state, wind statistics from the first to the fourth order were computed by using a horizontal- and time-averaging procedure. Horizontal averaging was performed in the x and y directions and time averaging over a period of 900 s with a frequency of 1 Hz. On Fig. 11, the good agreement between the Meso-NH model, ARPS model simulations (Dupont and Brunet 2008a) and measurements (Su et al. 1998) can be observed. It shows that Meso-NH is able to reproduce the well-known characteristics of turbulence under and above the canopy:

- the profile of longitudinal wind speed presents an inflexion point at the top of the trees.
- momentum flux, TKE and the variance of the three wind components are constant above the cover and then decrease dramatically within it, due to the effects of the drag force.

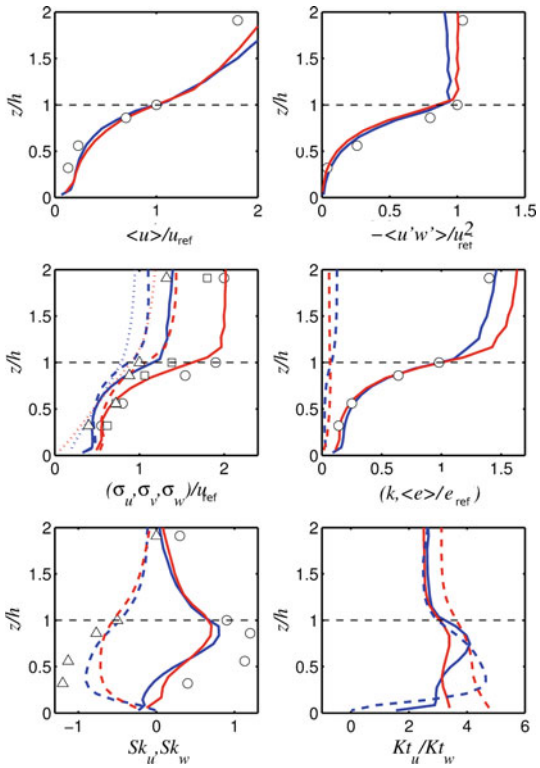

Fig. 11 Validation of Meso-NH model (*blue*) against ARPS (*red*) (Dupont and Brunet 2008b) and measurements (*black*) (Su et al. 1998) in a homogeneous forest canopy. Vertical profiles of mean horizontal wind velocity; momentum flux; standard deviations of the three wind components (σ_u: *solid line*, *empty circle*; σ_v: *long dashed line*, *empty square*; σ_w: *short-dashed line*, *empty triangle*); total TKE; skewnesses of u and w (Sk_u: *solid line*, *empty circle*; Sk_w: *dashed line*, *empty triangle*); Kurtosis of u and w (Kt_u: *solid line*, Kt_w: *dashed line*)

– the skewness of the longitudinal and vertical wind shows some asymmetry. There is a positively skewed longitudinal velocity and a negatively skewed vertical velocity. This can be explained by the dominance of organized sweeps over ejections on momentum transfer according to Poggi et al. (2004).

Statistical measurements made recently by Poggi and Katul (2010) within the canopy show the same behaviour as do our results. Thus, the implementation of the drag-force approach in Meso-NH shows its ability to correctly reproduce the main behaviour of the flow above and within a canopy layer.

References

Aumond P, Gauvreau B, Lac C, Masson V, Bérengier M (2012) Numerical predictions for environmental acoustics: simulation of atmospheric fields and integration in a propagation model. Invited paper, Proc Acoustics 2012 (joint SFA/IOA international congress), Nantes (F), 23–27 April

Bohrer G, Katul GG, Walko R, Avissar R (2009) Exploring the effects of microscale structural heterogeneity of forest canopies using large-eddy simulations. Boundary-Layer Meteorol 132:351–382

Bougeault P, Lacarrere P (1989) Parameterization of orography-induced turbulence in a mesobetascale model. Mon Weather Rev 117:1872–1890
Büttner G, Feranec J, Jaffrain G, Mari L, Maucha G, Soukup T (2004) The CORINE land cover 2000 project. EARSeL eProc 3(3):331–346
Cassiani M, Katul G, Albertson J (2008) The effects of canopy leaf area index on airflow across forest edges: large-eddy simulation and analytical results. Boundary-Layer Meteorol 126(3):433–460
Chamecki M, Meneveau C, Parlange M (2009) Large eddy simulation of pollen transport in the atmospheric boundary layer. J Aerosol Sci 40(3):241–255
Chow F, Weigel A, Street R, Rotach M, Xue M (2006) High-resolution large-eddy simulations of flow in a steep Alpine valley. Part I: Methodology, verification, and sensitivity experiments. J Appl Meteorol Climatol 45(1):63–86
Cuxart J, Bougeault P, Redelsperger JL (2000a) A turbulence scheme allowing for mesoscale and large-eddy simulations. Q J R Meteorol Soc 126:1–30
Cuxart J, Yague C, Morales G, Terradellas E, Orbe J, Calvo J, Fernández A, Soler M, Infante C, Buenestado P et al (2000b) Stable atmospheric boundary-layer experiment in Spain (SABLES 98): a report. Boundary-Layer Meteorol 96(3):337–370
Deardorff J (1980) Stratocumulus-capped mixed layers derived from a three-dimensional model. Boundary-Layer Meteorol 18(4):495–527
Déqué M, Dreveton C, Braun A, Cariolle D (1994) The ARPEGE/IFS atmosphere model: a contribution to the French community climate modelling. Clim Dyn 10:249–270
Dupont S, Brunet Y (2008a) Edge flow and canopy structure: a large-eddy simulation study. Boundary-Layer Meteorol 126(1):51–71
Dupont S, Brunet Y (2008b) Impact of forest edge shape on tree stability: a large-eddy simulation study. Forestry 81(3):299
Dupont S, Brunet Y, Finnigan J (2008) Large-eddy simulation of turbulent flow over a forested hill: validation and coherent structure identification. Q J R Meteorol Soc 134(636):1911–1929
Finnigan J (2000) Turbulence in plant canopies. J Fluid Mech 32(1):519–571
Irvine M, Gardiner B, Hill M (1997) The evolution of turbulence across a forest edge. Boundary-Layer Meteorol 84(3):467–496
Jiménez M, Cuxart J (2005) Large-eddy simulations of the stable boundary layer using the standard Kolmogorov theory: range of applicability. Boundary-Layer Meteorol 115(2):241–261
Junker F, Gauvreau B, Bérengier M, Cremezi-Charlet C, Blanc-Benon P, Cotté B, Ecotière D (2006) Classification of relative influence of physical parameters for long range acoustic propagation. Invited paper to Internoise 2006, Honolulu (EUA), December
Kanda M, Hino M (1994) Organized structures in developing turbulent flow within and above a plant canopy, using a large eddy simulation. Boundary-Layer Meteorol 68(3):237–257
Lafore J, Stein J, Asencio N, Bougeault P, Ducrocq V, Duron J, Fischer C, Hereil P, Mascart P, Pinty J, Redelsperger J, Richard E, de Arellano JVG (1998) The Meso-NH atmospheric simulation system. Part I: Adiabatic formulation and control simulations. Ann Geophys 16:90–109
Masson V, Seity Y (2009) Including atmospheric layers in vegetation and urban offline surface schemes. J Appl Meteorol Climatol 48:1377–1397
Mayhead G (1973) Some drag coefficients for British forest trees derived from wind tunnel studies. Agric Meteorol 12:123–130
Noilhan J, Planton S (1989) A simple parameterization of land surface processes for meteorological models. Mon Weather Rev 117(3):536–549
Otte T, Lacser A, Dupont S, Ching J (2004) Implementation of an urban canopy parameterization in a mesoscale meteorological model. J Appl Meteorol 43(11):1648–1665
Patton E, Shaw R, Judd M, Raupach M (1998) Large-eddy simulation of windbreak flow. Boundary-Layer Meteorol 87(2):275–307
Patton E, Sullivan P, Davis K (2003) The influence of a forest canopy on top-down and bottom-up diffusion in the planetary boundary layer. Q J R Meteorol Soc 129(590):1415–1434
Pimont F, Dupuy J, Scarella G, Caraglio Y, Morvan D (2006) Effects of small scale heterogeneity of vegetation on radiative transfer in forest fire. For Ecol Manag 234:S88
Poggi D, Katul G (2010) Evaluation of the turbulent kinetic energy dissipation rate inside canopies by zero- and level-crossing density methods. Boundary-Layer Meteorol 136:1–15
Poggi D, Katul G, Albertson J (2004) Momentum transfer and turbulent kinetic energy budgets within a dense model canopy. Boundary-Layer Meteorol 111(3):589–614
Shaw R, Schumann U (1992) Large-eddy simulation of turbulent flow above and within a forest. Boundary-Layer Meteorol 61(1):47–64

Shen S, Leclerc M (1997) Modelling the turbulence structure in the canopy layer. Agric For Meteorol 87(1): 3–25

Su H, Shaw R, Paw K, Moeng C, Sullivan P (1998) Turbulent statistics of neutrally stratified flow within and above a sparse forest from large-eddy simulation and field observations. Boundary-Layer Meteorol 88(3):363–397

Tomas S, Masson V (2006) A parameterization of third-order moments for the dry convective boundary layer. Boundary-Layer Meteorol 120(3):437–454

Weigel A, Chow F, Rotach M, Street R, Xue M (2006) High-resolution large-eddy simulations of flow in a steep Alpine valley. Part II: Flow structure and heat budgets. J Appl Meteorol Climatol 45(1):87–107

Weigel A, Chow F, Rotach M (2007) On the nature of turbulent kinetic energy in a steep and narrow Alpine valley. Boundary-Layer Meteorol 123(1):177–199